All-analytical semiclassical theory of spaser performance in a plasmonic nanocavity

Xiao-Lan Zhong and Zhi-Yuan Li*

Laboratory of Optical Physics, Institute of Physics, Chinese Academy of Sciences, Beijing 100190, China

(Received 1 April 2013; revised manuscript received 4 June 2013; published 1 August 2013)

Experimental approaches to manipulating light-matter interaction at the nanoscale level have quickly advanced in recent years, leading to the use of surface plasmon amplification by stimulated emission of radiation (spaser) in plasmonic nanocavities. Yet, a well-understood analytical theory to quantitatively explain certain characteristics of the spaser system has still been lacking and is greatly needed. Here, we develop an all-analytical semiclassical theory to investigate the energy exchange between active materials and fields and the spaser performance in a plasmonic nanocavity. The theory incorporates the four-level atomic rate equations in association with the classical oscillator model for active materials and Maxwell's equations for fields, thus allowing one to uncover the relationship between the characteristics of the spaser (the output power, saturation, and threshold) and the nanocavity parameters (quality factor, mode volume, loss, and spontaneous emission efficiency), atomic parameters (number density, linewidth, and resonant frequency), and external parameters (pumping rate). The semiclassical theory has been employed to analyze previous spaser experiments and shows that using a single gold nanoparticle plasmonic nanocavity to ignite the spaser is very difficult due to its high threshold. The theory can be commonly used in understanding and designing all novel microlaser, nanolaser, and spaser systems.

DOI: 10.1103/PhysRevB.88.085101 PACS number(s): 42.60.−v, 78.20.Ci, 42.55.−f, 78.20.Bh

I. INTRODUCTION

In recent years we have witnessed the rapid development of microprocessing technology, integrated optics, and nanophotonics.[1–3] One of the central issues, the interaction between light and active photonic and plasmonic nanostructured materials, has attracted extensive and intensive interest in research.[1–6] The capability to control light at the nanoscale level by these active nanostructures has given rise to a rich variety of physical phenomena, such as trapping and manipulation of photons in a resonant nanocavity,[1–3] coherent emission, transport, and amplification of surface plasmons,[4–6] giant local field enhancement,[7,8] compensation of metallic dissipation loss,[9,10] and amplification of gain.[11,12] These phenomena can be harnessed for building high-efficiency miniaturized photonic and optoelectronic devices. Through a multipronged effort, numerous theoretical and experimental works have been devoted to exploring novel ways to miniaturize traditional laser systems and realizing nanolasers with tiny footprints and low power consumption. Among them, photonic crystal nanocavity lasers[13–18] and plasmonic lasers[19–31] have stood out as two prominent routes toward this fundamental purpose. The former is based on localization and amplification of light within a semiconductor nanocavity with gain media, while the latter is based on so-called surface plasmon amplification by stimulated emission of radiation (spaser)[4,19] in plasmonic nanostructures incorporated with gain media.

In principle, the properties and performances of nanolasers are understood with the semiclassical physical model of harmonic oscillators coupled to electromagnetic fields. Yet, because the geometries of nanolasers are very complicated, involving many subtle nanoscale morphologic features, the electromagnetic fields of laser modes do not have simple spatial profiles, but rather they are far more complex than plane waves or Gaussian beams in traditional laser systems. As a result, it is not easy to describe the interaction of gain media with electromagnetic fields in a simple analytical way as in a traditional laser system.[32] Perhaps, for this reason up to now, researchers largely only employ numerical simulation methods, e.g., a finite-difference time-domain (FDTD) method, in combination with the atomic rate equations, the dipole approximation model, and Maxwell's equations, to investigate nanolasers in several realistic, active dielectric and plasmonic systems.[33–39] In contrast, the efforts to build some analytical models to solve the central issues of nanolaser performance are still very rare.[40–42] As is known, a simple, comprehensive, and still quantitatively accurate analytical theory can greatly help to better understand, explain, and predict all related and important issues of these complicated active nanolaser systems, making it easier to design novel systems with improved performance. In comparison, using only all-numerical simulations, although they provide technically accurate data about nanolaser performance, is insufficient to provide a clear overall physical picture about these central issues.

In this paper, we report our effort to construct an easy-to-understand, all-analytical semiclassical theory for nanolasers by taking into account the energy exchange between active materials and fields, power density conservation, spontaneous emission, and stimulated emission. The theory starts from the basic atomic rate equation in association with the classical oscillator model, considers various aspects of nanocavity parameters, atomic parameters, and external pumping parameters, and has a final form looking very similar to that for conventional lasers.[32] We will focus on plasmonic lasers, where the spaser takes place in a plasmonic nanocavity with active materials. The derived all-analytical semiclassical theory can explain the spaser effect in this plasmonic nanolaser system more clearly and precisely.

II. THEORETICAL MODEL AND ANALYTICAL SOLUTION

We consider a plasmonic nanocavity that is composed of a metallic core, providing plasmon resonance modes, surrounded by a dielectric shell containing active materials,

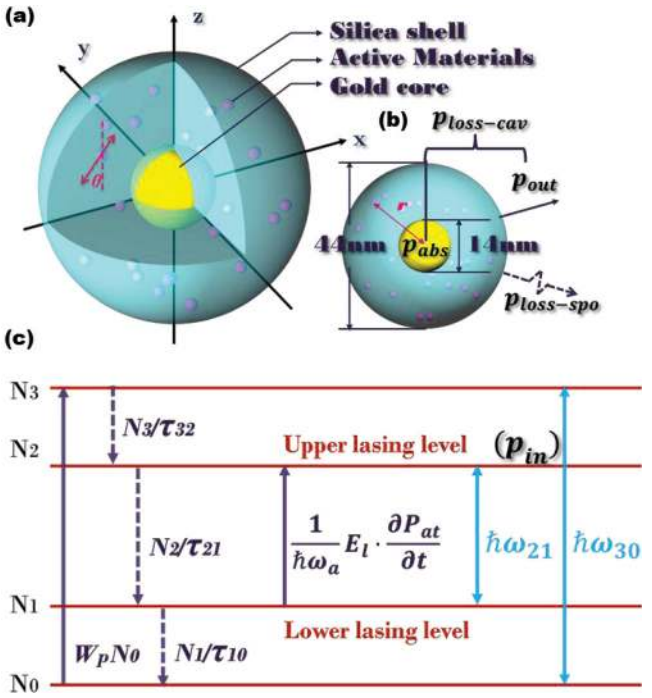

FIG. 1. (Color online) Schematic plot of the light-matter interaction of a general four-level atomic system with a metallic nanocavity. (a) Geometry of the plasmonic nanocavity, which is a core-shell nanoparticle consisting of a metallic core and dielectric shell doped with four-level atoms as active materials. Each atom is modeled as a radiation dipole. θ is the angle of the dipole polarization, and r is the distance between the dipole and the center of the metallic core. (b) Energy output from the plasmonic nanocavity, where $p_{\rm out}$ is the output laser power density, $p_{\rm abs}$ is the metallic absorption power density by the plasmonic cavity, and $p_{\rm loss-spo}$ is the loss of spontaneous emission power density. (c) Schematic of a general four-level atomic system that describes the spontaneous and stimulated radiation and various atomic transition parameters. The straight and dashed lines correspond to the radiative and nonradiative transitions, respectively. $p_{\rm in}$ is the storage power density by the upper lasing level.

providing gain. The active materials are described by a general four-level atomic system. The structure, as schematically illustrated in Figs. 1(a) and 1(b), can describe the gain and loss process happening in a general optical nanocavity very well. When the electrons are pumped from the ground-state level with a constant pump rate, spontaneous emission happens immediately. Due to the feedback effect by the surface plasmon resonance of the metallic core, it will cause stimulated emission until a steady state is reached. The schematic diagram of the atomic system is shown in Fig. 1(c), where level one and two are the lower and upper lasing levels, respectively. Under the dipole approximation, the active materials can be seen as dipoles. Our aim is to develop a methodology to describe the characteristics of light-matter interaction in this nanolaser system. Similar to conventional laser theory,[32] we consider atomic transitions in the current nanolaser system quantum mechanically and adopt the model of atomic rate equations to describe these transitions, while handling the radiation of electromagnetic field classically, whose motion follows Maxwell's equations. The interaction between atoms and fields is thus treated semiclassically. Such a semiclassical theory should yield a much more precise description and better prediction of the optical properties of these nanolaser systems than the usual classical theory, where the role of atoms comprising the active materials is described by the phenomenological parameter of dielectric permittivity.[7,8,11,12]

The occupation numbers of electrons at the atomic levels at each spatial point vary according to the atomic rate equations:[35–37]

$$\frac{dN_3}{dt} = W_P N_0 - \frac{N_3}{\tau_{32}}, \tag{1}$$

$$\frac{dN_2}{dt} = \frac{N_3}{\tau_{32}} + \frac{1}{\hbar\omega_a}E_l\cdot\frac{\partial P_{\rm at}}{\partial t} - \frac{N_2}{\tau_{21}}, \tag{2}$$

$$\frac{dN_1}{dt} = \frac{N_2}{\tau_{21}} - \frac{1}{\hbar\omega_a}E_l\cdot\frac{\partial P_{\rm at}}{\partial t} - \frac{N_1}{\tau_{10}}, \tag{3}$$

$$\frac{dN_0}{dt} = \frac{N_1}{\tau_{10}} - W_P N_0. \tag{4}$$

Equations (1) to (4) mean that an external excitation mechanism pumps electrons from the ground-state level (N_0) to the third level (N_3) at a certain pump rate (W_P), which is proportional to the pumping light intensity in the case of the optical pumping experiment. After a short lifetime (τ_{32}), electrons transfer nonradiatively into the upper lasing level, i.e., the second level (N_2). Electrons can be transferred from the upper to the lower lasing level, i.e., the first level (N_1), by spontaneous and stimulated emission. At last, electrons transfer quickly and nonradiatively from the first level (N_1) to the ground-state level (N_0). The lifetimes and energies of the upper and lower lasing levels are τ_{21}, E_2 and τ_{10}, and E_1, respectively. The center frequency of the radiation is $\omega_a = (E_2 - E_1)/\hbar$. E_l is the local electric field in the cavity, $P_{\rm at}$ is the electric polarization of atoms, and $\frac{1}{\hbar\omega_a}E_l\cdot\frac{\partial P_{\rm at}}{\partial t}$ is the induced radiation rate or excitation rate, depending on its sign. As time goes on, the system gradually reaches the steady state, which is described by $dN_i/dt = 0$. The populations at steady state can be easily solved and written as

$$N_{1,ss} = W_P N_0 \tau_{10}, \tag{5}$$

$$N_{2,ss} = W_P N_0 \tau_{21} - \frac{\omega\tau_{21}\varepsilon_0}{2\hbar\omega_a}\chi''_{\rm at}E_l^2, \tag{6}$$

$$N_{3,ss} = W_P N_0 \tau_{32}, \tag{7}$$

where $\chi''_{\rm at}$ is the imaginary part of the atomic polarizability.

The population difference between the lower and upper lasing level is

$$\Delta N_{12} = W_P N_0(\tau_{10} - \tau_{21}) + \frac{\omega\tau_{21}\varepsilon_0}{2\hbar\omega_a}\chi''_{\rm at}E_l^2. \tag{8}$$

Following the classical harmonic oscillator model, the polarization $P_{\rm at}$ in the presence of an electric field obeys locally the following equation of motion:

$$\frac{d^2P_{\rm at}(t)}{dt^2} + \Delta\omega_a\frac{dP_{\rm at}(t)}{dt} + \omega_a^2 P_{\rm at}(t) = \Gamma_a\Delta N(t)E_l(t), \tag{9}$$

where $\Delta\omega_a$ is the linewidth of atomic transition frequency and Γ_a is the coupling strength of the polarization to the external electric field. The expression Γ_a is $3\omega_a\varepsilon_h\lambda^3\gamma_{\rm rad}/4\pi$, where $\gamma_{\rm rad}$

is the radiative decay rate, ε_h is the dielectric constant of host material, and λ is the radiation wavelength.

From Eq. (9), the polarization can be written as

$$P_{\text{at}} = \frac{\Gamma_a(N_1 - N_2)}{\left(\omega_a^2 - \omega^2 + j\omega\Delta\omega_a\right)} E_l. \tag{10}$$

According to the power density conservation, the storage power density by the upper lasing level p_{in} is equal to the sum of the output power density p_{out}, the absorption power density by the cavity p_{abs}, and the loss of spontaneous emission power density $p_{\text{loss-spo}}$. The output power density and the absorption power density constitute the loss of cavity power density $p_{\text{loss-cav}}$. The above relationship can be expressed as

$$p_{\text{in}} = p_{\text{out}} + p_{\text{abs}} + p_{\text{loss-spo}}, \tag{11}$$

and

$$p_{\text{loss-cav}} = p_{\text{out}} + p_{\text{abs}}. \tag{12}$$

Due to the electronic pumping, the power density, which can be seen and used by the third level, can be written as

$$p_{\text{pump}} = W_P N_0 \hbar\omega_{30}. \tag{13}$$

We introduce a parameter called quantum efficiency η_{qe} so that the storage power density by the upper lasing level p_{in} is

$$p_{\text{in}} = \eta_{\text{qe}} \times p_{\text{pump}}. \tag{14}$$

As is known, the power loss of the cavity is proportional to $\omega\varepsilon_0 E_l^2 V_m/Q$, where ω is the resonance frequency of the cavity, V_m is the mode volume, and Q is the quality factor (Q factor) of the cavity. This is the standard definition of the Q factor of a resonant cavity. We bring in another parameter called the cavity loss coupling strength coefficient η_F, which strongly depends on the geometric and material parameter of the cavity so that the total power loss of the cavity can be written as

$$P_{\text{loss-cav}} = \eta_F \times \frac{\omega\varepsilon_0 E_l^2 V_m}{Q}, \tag{15}$$

and the power density loss is $p_{\text{loss-cav}} = P_{\text{loss-cav}}/V_c$, where V_c is the cavity volume. It is obvious that a larger value of η_F means easier loss of energy power from the cavity.

The spontaneous emission power is only relevant to the population of the upper lasing level, and we can obtain the spontaneous emission power density in the follow expression

$$p_{\text{spo}} = \frac{N_{2,ss}\hbar\omega_a}{\tau_{21}}. \tag{16}$$

We notice that the spontaneous emission power is proportional to the upper lasing level population; however, not all of the spontaneous emission power runs away from the cavity. Most of them are either used to excite stimulated emission or absorbed by the cavity. The escaped spontaneous emission power density from the cavity can be defined as

$$p_{\text{loss-spo}} = \eta_{\text{spo}} \times p_{\text{spo}}, \tag{17}$$

where η_{spo} is called the loss of spontaneous emission efficiency. Obviously, a larger value of η_{spo} means the greater loss of spontaneous emission power from the cavity and simultaneously less conversion of this power into the useful laser energy power for the cavity.

Taking Eqs. (12), (14), (15), and (17) into consideration, we have

$$\eta_{\text{qe}} \times p_{\text{pump}} = \eta_F \times \frac{\omega\varepsilon_0 E_l^2 V_m}{Q V_c} + \eta_{\text{spo}} \times p_{\text{spo}}. \tag{18}$$

Taking the relevant equations into Eq. (18), then we have

$$\eta_{\text{qe}} \times W_P N_0 \hbar\omega_{30} = \eta_F \times \frac{\omega\varepsilon_0 E_l^2 V_m}{Q V_c} + \eta_{\text{spo}} \times \frac{N_{2,ss}\hbar\omega_a}{\tau_{21}}. \tag{19}$$

We consider the original definition of polarization that is shown below

$$P_{\text{at}} = \chi_{\text{at}}\varepsilon_0 E_l = (\chi'_{\text{at}} + j\chi''_{\text{at}})\varepsilon_0 E_l, \tag{20}$$

where χ'_{at} is the real part of the atomic polarizability.

The above formulae can be combined together to offer a solution for various optical properties for the nanolaser system, after some tedious, but straightforward, algebraic manipulations. We start from the quantity of atomic polarizability χ_{at}. For the sake of simplicity of the discussion, we define three parameters:

$$\rho_1 = Q V_c \eta_{\text{spo}} \omega_a \varepsilon_0 \left[\frac{4\omega_a^2(\omega_a - \omega)^2 + \omega^2\Delta\omega_a^2}{\Delta\omega_a}\right], \tag{21a}$$

$$\rho_2 = Q V_c \Gamma_a W_P N_0 \omega(\eta_{\text{spo}}\omega_a\tau_{10} - \eta_{\text{qe}}\omega_{30}\tau_{21}) - 2V_m\eta_F\omega_a\varepsilon_0\left[\frac{4\omega_a^2(\omega_a - \omega)^2 + \omega^2\Delta\omega_a^2}{\Delta\omega_a}\right], \tag{21b}$$

$$\rho_3 = 2\Gamma_a W_P N_0 V_m \eta_F \omega_a \omega(\tau_{21} - \tau_{10}). \tag{21c}$$

By using Eqs. (6), (10), (19), and (20), χ''_{at} can be written as

$$\chi''_{\text{at}} = -\frac{\rho_2 + \sqrt{\rho_2^2 - 4\rho_1\rho_3}}{2\rho_1}. \tag{22}$$

Equation (22) represents the absorbing (or amplifying) part of the atomic response.

Respectively, χ'_{at} and the local electric field can be written as

$$\chi'_{\text{at}} = \frac{2\omega_a(\omega - \omega_a)\chi''_{\text{at}}}{\omega\Delta\omega_a}, \tag{23}$$

$$E_l^2 = \frac{(\eta_{\text{qe}} \times \hbar\omega_{30} - \eta_{\text{spo}} \times \hbar\omega_a) W_P N_0}{(\eta_F \times \omega\varepsilon_0 V_m/Q V_c - \eta_{\text{spo}} \times \omega\varepsilon_0\chi''_{\text{at}}/2)}. \tag{24}$$

If the radiation frequency ω_a is equal to the cavity resonance frequency ω, the equations will become much simpler.

Considering the dipole approximation and the tiny nanocavity volume, the absorption power density of the metallic core can be written as

$$p_{\text{abs}} = \tfrac{1}{2}\varepsilon_0\omega\chi''_{\text{host}}E_l^2. \tag{25}$$

If the power loss density of the cavity $p_{\text{loss-cav}}$ is larger than the absorption power density of the metallic core p_{abs}, which means that the cavity constant η_F is larger than $\chi''_{\text{host}}V_c Q/2V_m$, the laser can output from the cavity. We will discuss how to calculate the cavity constant η_F later. Now, we can deduce the output power density of the nanolaser system, which can be

written as

$$p_{\text{out}} = \frac{(2\eta_F V_m - Q\chi''_{\text{host}})}{2Q}\omega\varepsilon_0 E_l^2. \quad (26)$$

The output power of the active nanocavity is also proportional to the laser field intensity within the cavity. Until now, we have used the all-analytical semiclassical theory for quantitatively describing the spaser system. The theoretical model has considered all concerned parameters, and it is a generic model enabling us to solve and explain a variety of complex spaser and nanolaser systems. In order to show a clearer physical image, we will give a detailed analysis in the following section.

We notice that in the above derivation of the all-analytical semiclassical theory, the local electric field E_l within the plasmonic nanocavity has been assumed to be a constant. This approximation is reasonable for a nanocavity whose size is much smaller than the radiation wavelength, e.g., the spherical nanoparticle in Ref. 24 that will be discussed in the following section. In this simple situation, classical electrostatics indicates that the inner electric field, parallel to the external electric field, is almost uniform everywhere within the spherical nanoparticle. In the more complicated situation for a general nanocavity whose size is not very tiny and whose geometric shape is not a regular sphere, the general framework of our semiclassical theory still holds true. This is because many cavity parameters, such as the cavity loss coupling strength coefficient η_F, Q factor Q, cavity volume V_c, mode volume V_m, the resonance frequency ω, and the loss of spontaneous emission efficiency η_{spo}, are concepts applicable to various situations of nanolaser, rather than only to the simple spherical nanoparticle considered in Ref. 24. In fact, these parameters are case sensitive, and they need to be determined in each case. The thing that needs significant modification is the local field E_l, which now is not a constant but has a spatial distribution, and its interaction with the electric polarization of atoms, which is described by $E_l \cdot \frac{\partial P_{\text{at}}}{\partial t}$. The detailed modal profile of the nanocavity laser mode must be taken into account, and the contribution of each atomic dipole within the modal field to the energy exchange must be weighted appropriately. Taking into account this modification, the semiclassical nanolaser theory can be applicable to a general nanolaser system with sufficient quantitative precision.

III. ANALYTICAL AND NUMERICAL RESULTS AND DISCUSSIONS

The above equations that constitute the all-analytical semiclassical theory involve many parameters, most of which are adjustable. We divide these parameters into three parts: cavity parameters, atomic parameters, and external input parameters. As these parameters have encompassed all the geometric and physical details of the nanocavity system, the theory is quite general and can handle various types of nanolasers and various optical problems. The quantum efficiency η_{qe}, the coupling strength of atomic polarization to the external electric field Γ_a, the lifetime of each level τ_{21}, τ_{10}, and τ_{32}, the transition frequency ω_a and ω_{30}, and the linewidth of atomic transition frequency $\Delta\omega_a$ belong to atomic parameters. The cavity loss coupling strength coefficient η_F, Q factor, Q, cavity volume V_c, mode volume V_m, the resonance frequency ω, even the loss of spontaneous emission efficiency η_{spo} are cavity parameters. The pump rate W_P is the only external input parameter. Also, there are some constant quantities in this system, e.g., the total population density N_0.

To obtain clear physical images and insights about the relationship between the spaser properties and the cavity parameters as well as the external excitation parameters, we choose several parameters as reported in Ref. 24. The number of dye molecules per nanoparticle is 2700. The core and shell diameters of the plasmonic cavity are 14 and 44 nm, respectively, so the cavity volume V_c is 1.436×10^{-24} m^3, and the total population density N_0 is 6.255×10^{25} m^{-3}. The radiation frequency ω_a is 3.5565×10^{15} Hz, and the corresponding wavelength is 530 nm, which is close to the resonance wavelength of the cavity. The linewidth of the transition frequency $\Delta\omega_a$ is around $0.04\omega_a$. The lifetime τ_{10}, τ_{21}, and τ_{32} are chosen as 10^{-9} s, 10^{-8} s, and 10^{-9} s, respectively. The coupling strength of P_{at} to the external electric field Γ_a is taken to be 10^{-4} C^2/kg according to Ref. 35. In our calculations, we find that Γ_a does not have a direct influence on the local electric field, the atomic polarizability, or even the output power density. Instead, it is the nature of the atomic system, so we will not discuss the influence of Γ_a in this paper.

We first consider the relationship between the local electric field and cavity parameters. The results are shown in Fig. 2 by color contour maps. Each time, we only discuss the relationship between two various parameters and the local electric field. Here, the pumping rate W_P, the Q factor, the cavity loss coupling strength coefficient η_F, and the loss spontaneous emission efficiency η_{spo} are fixed as 10^4 s^{-1}, 10, 3, and 6%, respectively. From Figs. 2(a) to 2(c), we find that the local electric field increases with the increase of W_P and Q factor, and with the decrease of η_F and η_{spo}. The relationship between these four parameters and the local electric field can be described by Eq. (24). From Figs. 2(a) and 2(e), we see that when η_{spo} is large enough, i.e., when most of the spontaneous emission does not participate in the lasing action, the local electric field can achieve saturation phenomenon with the increase of W_P and the Q factor. Otherwise, the saturation phenomenon cannot happen easily. From Fig. 2(b), we find that when the Q factor is small enough, i.e., when the loss of cavity is large, the local electric field can also achieve saturation phenomenon with W_P increasing. From Figs. 2(c), 2(d), and 2(f), the relationship between η_F and the local electric field is shown clearly. When η_F increases, the local electric field decreases. Note that a larger local electric field does not necessarily mean a higher lasing output power because of the absorption of the cavity, i.e., the absorption of the metallic core.

As is mentioned above, χ''_{at} means the absorbing (or amplifying) part of the atomic response, and it can directly describe the gain and loss of the system. Due to the complex expression of χ''_{at} by Eq. (22), it is hard to know its quantitative relationship with the cavity parameters directly. With the aid of computer calculation, we obtain some results as shown in Fig. 3. From Figs. 3(a) to 3(f), we find that χ''_{at} increases with the increase of W_P, η_F, η_{spo}, and with the decrease of the Q factor. The results are quite different from Fig. 2, and this means the

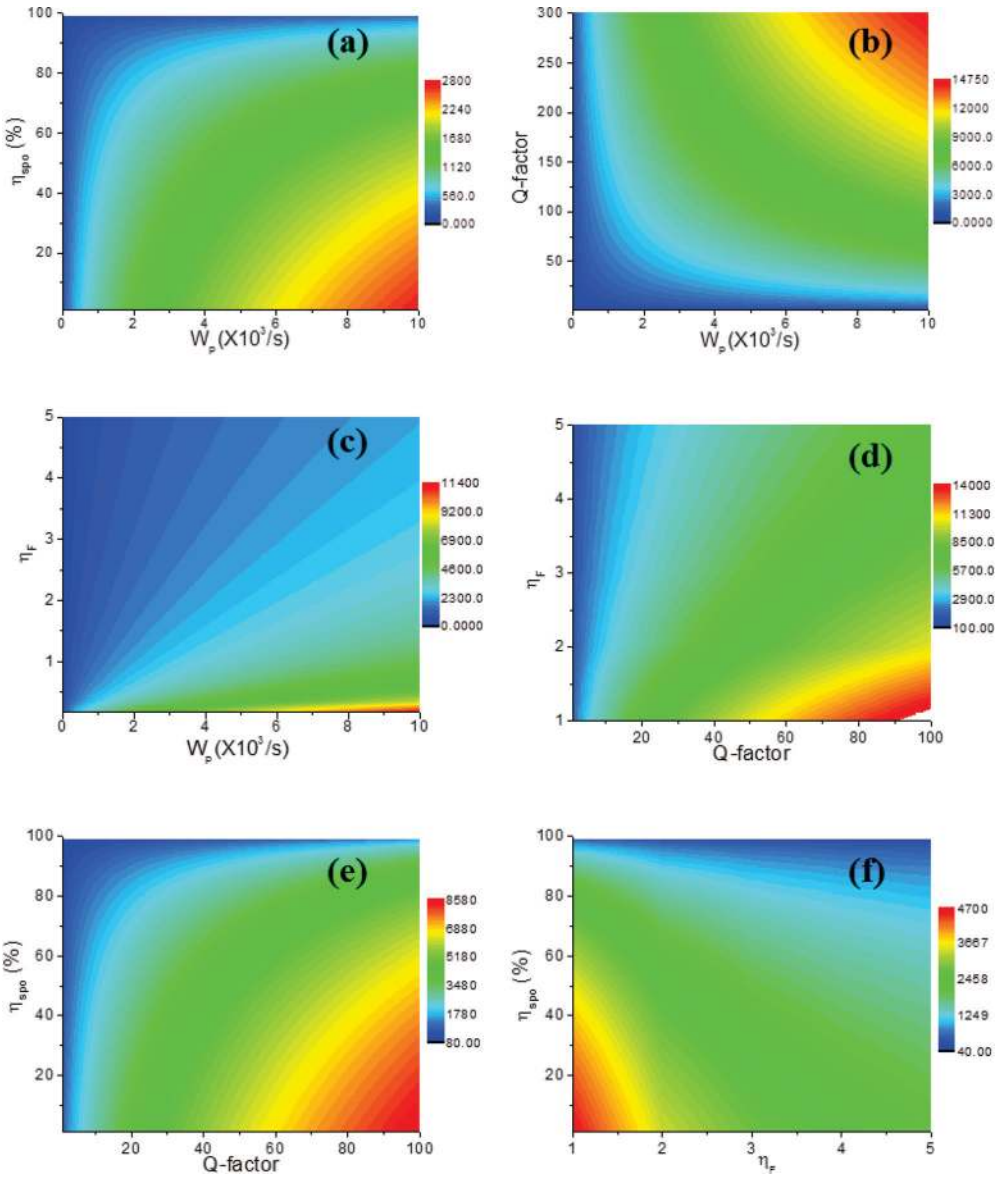

FIG. 2. (Color online) Contour maps of the local electric field amplitude E_l (V/m) as functions of various cavity parameters. (a) E_l as functions of pumping rate W_p and $\eta_{\rm spo}$; (b) E_l as functions of W_p and the Q factor; (c) E_l as functions of W_p and η_F; (d) E_l as functions of the Q factor and η_F; (e) E_l as functions of the Q factor and $\eta_{\rm spo}$; and (f) E_l as functions of η_F and $\eta_{\rm spo}$.

absorbing (or amplifying) part of the atomic response does not have a direct relation with the local electric field. From Figs. 3(a) and 3(c), we find that the influences of η_F and $\eta_{\rm spo}$ on $\chi''_{\rm at}$ are not obvious, because of the huge influences of pumping rate. We also find that when $\eta_{\rm spo}$ is large enough, i.e., when most of the spontaneous emission does not participate in the lasing action, $\chi''_{\rm at}$ can achieve the saturation phenomenon with the Q factor increasing. From Figs. 3(c), 3(d), and 3(f), the relationship between η_F and $\chi''_{\rm at}$ is shown clearly. When η_F increases, $\chi''_{\rm at}$ increases. This interesting phenomenon here is different from long-held general knowledge: A larger local electric field does not necessarily mean a larger gain for the nanocavity.

Next, we discuss an important quantity of much concern: the output power density $p_{\rm out}$ of the nanolaser system. This is a characteristic indicator for describing a laser system. The results are shown in Fig. 4. From Figs. 4(a) to 4(f), we find that the output power density increases with increasing of pumping rate and η_F and with decreasing of the Q factor and $\eta_{\rm spo}$. What is more, from the shaded parts of Figs. 4(b) and 4(c), we find that sometimes no matter how large the pumping rate is, there is still no output power density. At first glance, this may seem odd because as long as the gain is larger than the loss, there should be laser output, and the critical value of the pumping rate corresponds to the threshold. However, if we think over it more closely, we can find it is not difficult to explain. This spaser system is different from the traditional laser system because the cavity loss comes from the metallic absorption and the loss of spontaneous emission. Whether the metallic absorption or the loss of spontaneous emission, both of them are related to the local electric field, and the local electric field is proportional to the pumping rate, which means with increasing the pumping

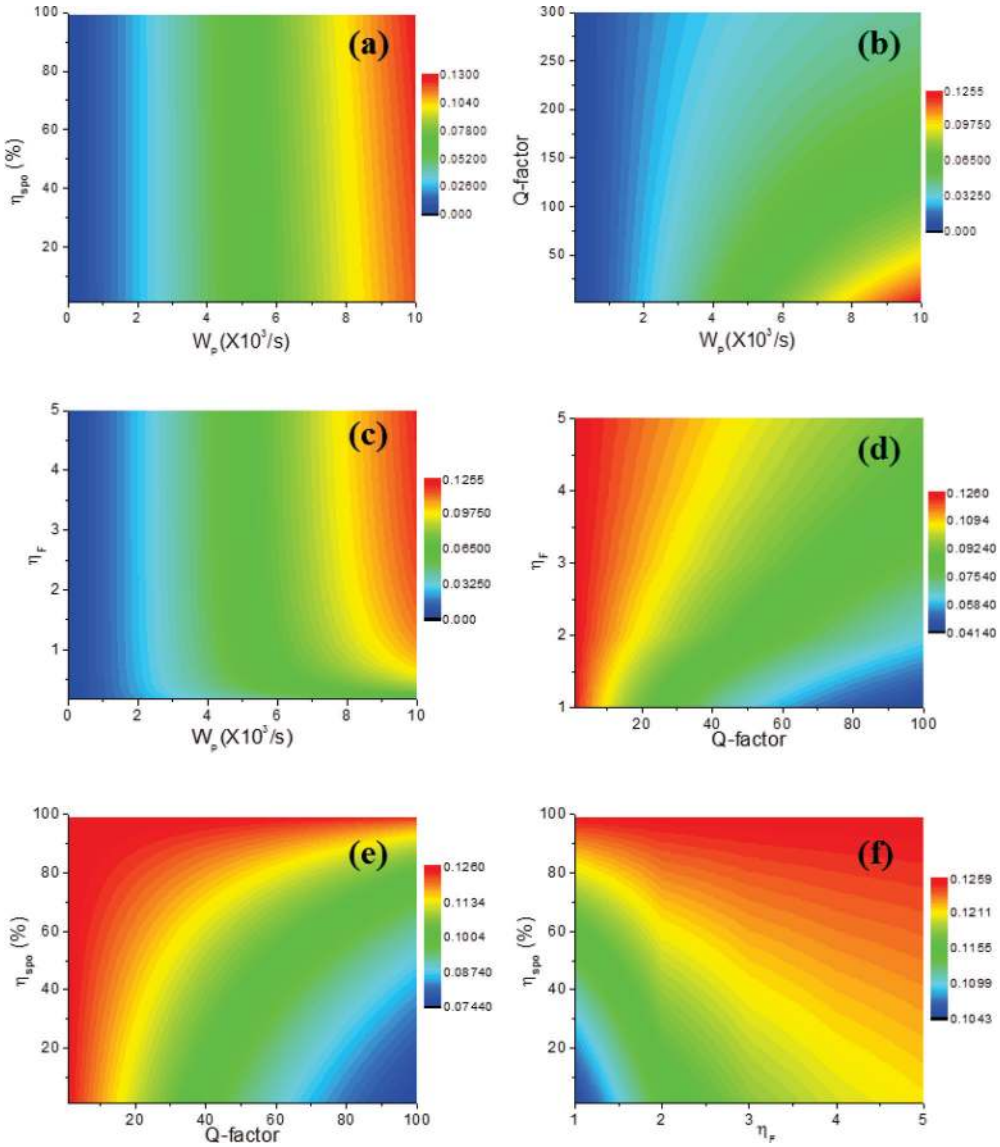

FIG. 3. (Color online) Contour maps of the imaginary part of atomic polarizability χ''_{at} as functions of various cavity parameters. (a) χ''_{at} as functions of pumping rate W_p and η_{spo}; (b) χ''_{at} as functions of W_p and the Q factor; (c) χ''_{at} as functions of W_p and η_F; (d) χ''_{at} as functions of the Q factor and η_F; (e) χ''_{at} as functions of the Q factor and η_{spo}; and (f) χ''_{at} as functions of η_F and η_{spo}.

rate, the loss also increases. The threshold of the spaser system comes from the cavity characteristics, i.e., the Q factor and η_F instead of large enough pumping rate. From Fig. 4(a), we note that when η_{spo} is large enough, i.e., most of the spontaneous emission does not join in the lasing action, the saturation phenomenon still exists, and the output power density can achieve saturation phenomenon with the pumping rate increasing. However, from Fig. 4(b), we can also find the similar saturation phenomenon only if the Q factor is less than the threshold. Focusing on the shaded region in Figs. 4(b) to 4(f), we obtain some important conclusions. As is known, the larger Q factor means the smaller cavity loss, and the larger η_F corresponds to the easier loss of energy power from the cavity. The function of the Q factor and η_F are opposite in influencing the performance of the spaser. From Eqs. (11) and (12), we can find that $p_{out} = p_{loss-cav} - p_{abs}$. As is mentioned above, both the metallic absorption and the loss of spontaneous emission are related to the local electric field intensity, either directly or indirectly. Therefore, this spaser system shows a threshold related with cavity parameters, i.e., Q factor and η_F.

To have a clarified physical image to illustrate the nature of the plasmonic nanocavity, we calculate the relationship between power density, the Q factor, and η_F. The results are shown in Fig. 5. From Figs. 5(a) to 5(d), the power densities are $p_{loss-cav}$, p_{abs}, and $p_{loss-spo}$, and the needed threshold power density of the plasmonic nanocavity p_{thr}, where $p_{thr} = p_{abs} + p_{loss-spo}$. From Eqs. (15) and (25), we find that both $p_{loss-cav}$ and p_{abs} are proportional to the local electric field intensity. The calculation results show the same phenomena in Figs. 5(a) and 5(b). From Fig. 5(c), we observe that $p_{loss-spo}$ increases with increasing η_F and with decreasing Q factor. From Eq. (11), we can find when p_{in} is larger than p_{thr}, the laser can output from the spaser system. In our model, p_{in} is equal to 2.3458×10^{11} W/m^3, which is marked in Fig. 5(d).

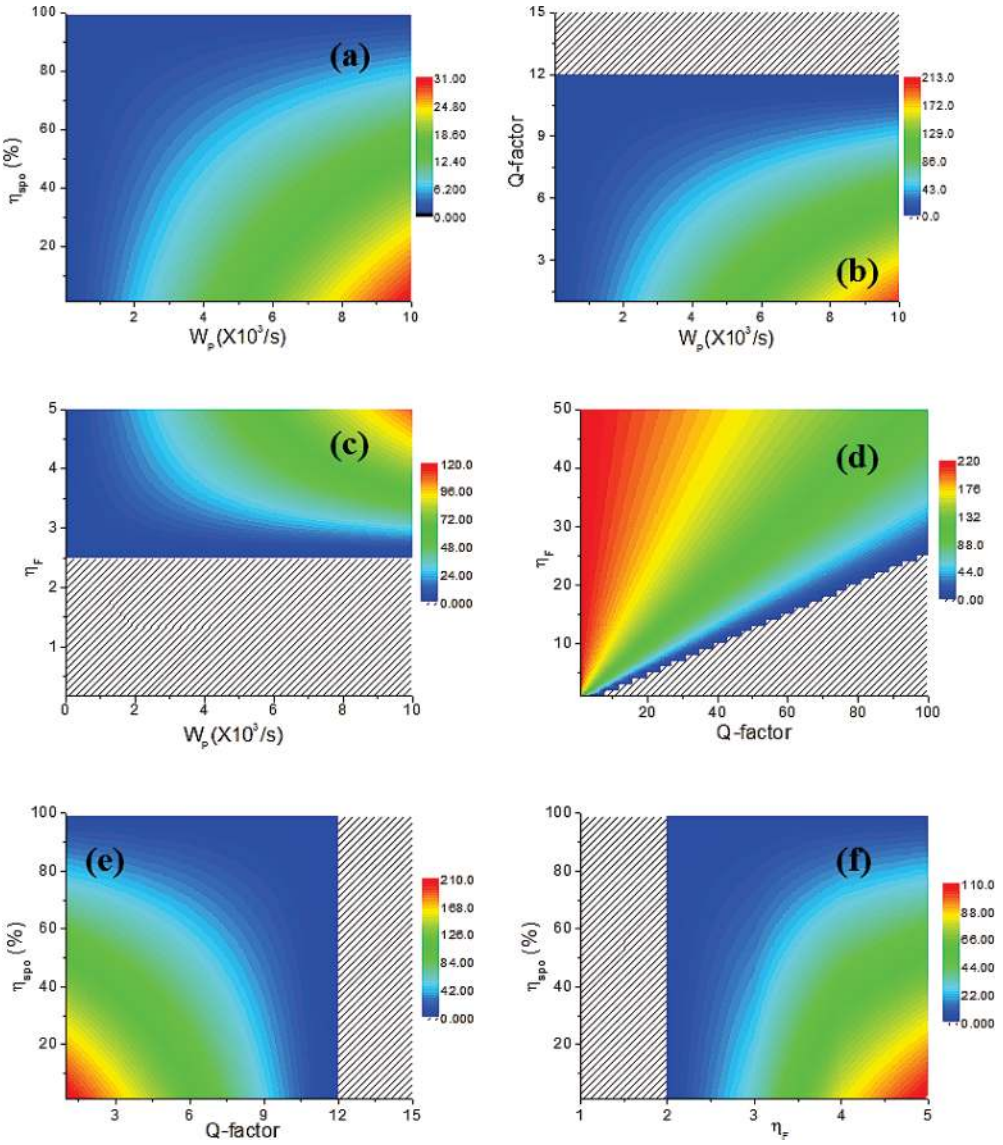

FIG. 4. (Color online) Contour maps of the laser output power density p_{out} (GW/m^3) as functions of various cavity parameters. (a) p_{out} as functions of the pumping rate W_p and η_{spo}; (b) p_{out} as functions of W_p and the Q factor; (c) p_{out} as functions of W_p and η_F; (d) p_{out} as functions of the Q factor and η_F; (e) p_{out} as functions of the Q factor and η_{spo}; (f) p_{out} as functions of η_F and η_{spo}. The shaded regions indicate that the output power density is zero.

Compared with Fig. 4(c), we find that when p_{thr} is larger than 2.3458×10^{11} W/m^3, the output power density is zero.

Another famous phenomenon that is often a concern is the population difference saturation. Using the all-analytical semiclassical theory, we can obtain the relationship between population saturation and pumping rate. The result is shown in Fig. 6. Here, the Q factor, η_F and η_{spo} are fixed as 10, 3, and 6%, respectively. From Fig. 6, we note that when the pumping rate increases, the population difference gradually becomes larger and larger until the saturation phenomenon happens.

IV. APPLICATION TO ANALYSIS OF PRACTICAL EXPERIMENTS

To further illustrate the power of the all-analytical semiclassical theory in handling the practical problems of nanolasers, we consider the experiments of Noginov *et al.*,[24] which present the first demonstration of the spaser. The spaser system is a plasmonic core-shell nanoparticle, which is composed of a gold core (diameter 14 nm), providing plasmon modes, surrounded by a silica shell (thickness 15 nm) containing the organic dye Oregon Green 488 (OG-488; density 6.25×10^{19} cm^{-3}), providing gain. In the experiment, the spectral and temporal characteristics of light leaking from the particles suspended in solution when optically pumped by nanosecond laser were measured. The narrowing of the radiation linewidth and linear increase of the magnitude of the resonant peak were observed and attributed to the ignition of the spaser from a single plasmonic nanoparticle, instead of from a collective group of nanoparticles.[24] However, this point has raised controversy, and is our target of theoretical evaluation by using the all-analytical semiclassical theory. To solve this

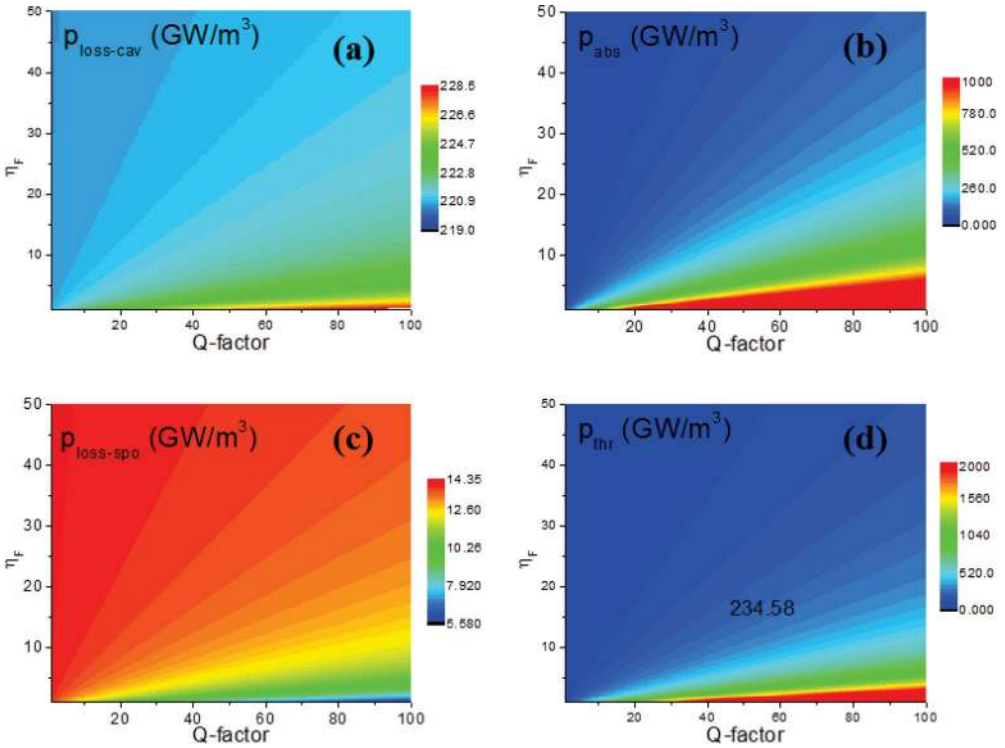

FIG. 5. (Color online) Contour plot of various power densities of the active plasmonic nanocavity as functions of the Q factor and η_F. (a) The loss of cavity power density $p_{\text{loss}-\text{cav}}$; (b) the absorption power density of the metallic core p_{abs}; (c) the loss of spontaneous emission power density $p_{\text{loss}-\text{spo}}$; and (d) the needed threshold power density of the nanocavity p_{thr}.

problem theoretically, we adopt a model as schematically depicted in Fig. 1, where the geometric parameters of the nanoparticle are explicitly shown.

To quantitatively handle this spaser problem, we first employ the FDTD method to calculate various cavity parameters. Considering the dipole approximation method, these OG-488 four-level atoms can be seen as dipoles that distribute uniformly around the metallic particle. Through the FDTD calculation, we obtain the single-dipole emission power P_0. The single-dipole emission power is an external parameter related to the pumping rate. The initial power density then can be written as $p_{\text{in}} = N_0 P_0$, and the pumping rate can be written as $W_P = P_0/\eta_{\text{qe}} \times \hbar\omega_{30}$. Taking into account the atomic parameters, we obtain $P_0 \approx 1.46 \times 10^{-15}$ W and $W_P \approx 4 \times 10^3$ s^{-1}. Next, we determine the loss spontaneous emission efficiency η_{spo}. Considering the different positions and dipole polarization angles, we take the average of the radiation power and calculate the value of η_{spo}. The dipole radiation power $P_{\text{rad}}(\theta, r)$ shows resonance at $\theta = 90^\circ$, where the loss of spontaneous emission of the spaser system becomes negligible. Considering different positions and angles, we take average of the radiation power and calculate the loss of spontaneous emission efficiency, which is $\eta_{\text{spo}} \approx 6\%$. The Q factor of this plasmonic cavity structure is about 10, and the modal volume is about 4.831×10^{-6} μm^3. The absorption power P_{abs0} by the metallic particle can also be calculated by FDTD method with a single-dipole source. Considering different positions and angles, we also need to take average of the absorption power. We obtain $\overline{P_{\text{abs0}}} \approx 9.448 \times 10^{-14}$ W, and the total absorption power density $p_{\text{abs}-\text{fdtd}} = N_0 \overline{P_{\text{abs0}}} \approx 5.91 \times 10^{12}$ W/m^3.

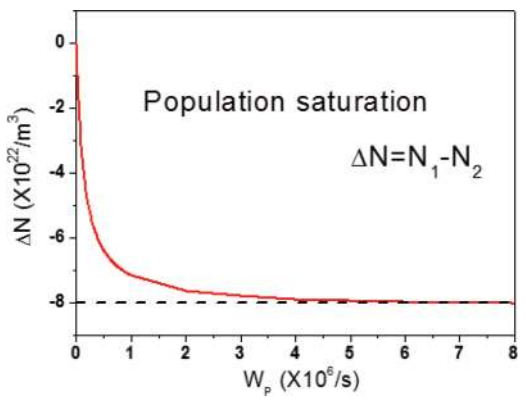

FIG. 6. (Color online) The relationship between the population difference and pumping rate.

From now on, the only unknown value is the cavity loss coupling strength coefficient η_F. From the above complete semiclassical theory, we have the relationship between absorption power density $p_{\text{abs}-\text{theory}}$ and η_F when other quantities are fixed. From the FDTD method, we have the determined total absorption power density, $p_{\text{abs}-\text{fdtd}}$ which is shown above. For the same system, no matter which method we use, either the all-analytical semiclassical theory or all-numerical simulation method, the total absorption power density is determined. Comparing the numerical results with the all-analytical theoretical results, we can always find $p_{\text{abs}-\text{theory}} = p_{\text{abs}-\text{fdtd}}$, which corresponds with the only determined η_F.

Through calculation, we determine $\eta_F = 0.04$ in this system. Recalling Fig. 4(d), we find that in that case, there is no output power density of the spaser from this plasmonic system. The measurement results in Ref. 24 are more likely not related with the spaser for a single plasmonic nanocavity. Instead, the observed laser performance (sharply narrowing the spectral response of emission light) might be attributed to other factors, such as random lasers due to the collective action of a group of metal nanoparticles. Our all-analytical semiclassical theory strongly suggests that in order to observe the spaser in this single plasmonic nanocavity, the atomic density of gain materials must be increased by two orders of magnitude so that a sufficiently large gain could be achieved.

V. CONCLUSIONS

We have investigated the interaction between light and the four-level atomic system embedded within a metallic particle and the spaser properties of this active plasmonic nanocavity system. By solving the coupled equations encompassing the atomic rate equation, the classical oscillator model, and Maxwell's equations and introducing several parameters that merely depend on the geometric and physical properties of the nanocavity, we have constructed an all-analytical semiclassical theory for describing the energy exchange between active materials and fields, light emission, and spaser performance in the plasmonic nanocavity. The theory incorporates the atomic rate equation in association with the classical oscillator model for active materials and Maxwell's equations for fields, thus allowing one to uncover the relationship between the characteristics of the spaser (the output power, saturation, and threshold) and the nanocavity parameters (quality factor, mode volume, loss, and spontaneous emission efficiency), atomic parameters (number density, linewidth, and resonant frequency), and external parameters (pumping rate). As a result, the all-analytical semiclassical theory can handle various nanocavity systems (semiconductor nanocavity, plasmonic nanocavity, and semiconductor nanowires) consisting of various active materials (atoms, molecules, ions, and semiconductors).

Through detailed calculation and analysis, several remarkable things about the spaser performance are discovered. The spaser system has all the characteristics of the traditional laser system, e.g., the saturation phenomenon and the threshold. The semiclassical theory has been employed to analyze previous spaser experiments and shows that using a single gold nanoparticle plasmonic nanocavity to ignite the spaser is very difficult due to its high threshold. As the all-analytical semiclassical theory has a simple formalism that looks like the conventional laser theory, it can offer an easy-to-understand yet sufficiently accurate means to explain the behavior of the spaser in plasmonic nanocavities and will be very useful in designing novel spaser devices with high performance. Furthermore, as this universal theory has involved many model parameters, it is expected that the theory can be applicable to many different microlaser, nanolaser, and spaser systems.

ACKNOWLEDGMENTS

This work is supported by the 973 Program of China (No. 2011CB922002 and No. 2013CB632704) and the Knowledge Innovation Program of the Chinese Academy of Sciences (No. Y1V2013L11).

*lizy@aphy.iphy.ac.cn

[1] S. Noda, A. Chutinan, and M. Imada, Nature (London) **407**, 608 (2000).
[2] K. J. Vahala, Nature (London) **424**, 839 (2003).
[3] Z.-Y. Li, Front. Phys. **7**, 601 (2012).
[4] D. J. Bergman and M. I. Stockman, Phys. Rev. Lett. **90**, 027402 (2003).
[5] A. V. Akimov, A. Mukherjee, C. L. Yu, D. E. Chang, A. S. Zibrov, P. R. Hemmer, H. Park, and M. D. Lukin, Nature (London) **450**, 402 (2007).
[6] M. I. Stockman, Opt. Express **19**, 22029 (2011).
[7] Z. Y. Li and Y. Xia, Nano Lett. **10**, 243 (2010).
[8] S. Y. Liu, J. Li, F. Zhou, L. Gan, and Z. Y. Li, Opt. Lett. **36**, 1296 (2011).
[9] Y.-H. Chen, J.-F. Li, M.-L. Ren, B.-L. Wang, J.-X. Fu, S.-Y. Liu, and Z.-Y. Li, Appl. Phys. Lett. **98**, 261912 (2011).
[10] B. Peng, Q. Zhang, X. Liu, Y. Ji, H. V. Demir, C. H. A. Huan, T. C. Sum, and Q. Xiong, ACS Nano **6**, 6250 (2012).
[11] D. B. Li and C. Z. Ning, Phys. Rev. B **80**, 153304 (2009).
[12] X. L. Zhong and Z. Y. Li, J. Opt. **14**, 055002 (2012).
[13] O. Painter, R. K. Lee, A. Scherer, J. D. O'Brien, P. D. Dapkus, and I. Kim, Science **284**, 1819 (1999).
[14] H. G. Park, S. H. Kim, S. H. Kwon, Y. G. Ju, J. K. Yang, J. H. Baek, S. B. Kim, and Y. H. Lee, Science **305**, 1444 (2004).
[15] H. Altug, D. Englund, and J. Vuckovic, Nat. Phys. **2**, 484 (2006).
[16] S. Matsuo, A. Shinya, T. Kakitsuka, K. Nozaki, T. Segawa, T. Sato, Y. Kawaguchi, and M. Notomi, Nat. Photon. **4**, 648 (2010).
[17] B. Ellis, M. A. Mayer, G. Shambat, T. Sarmiento, J. Harris, E. E. Haller, and J. Vuckovic, Nat. Photon. **5**, 297 (2011).
[18] A. Tandaechanurat, S. Ishida, D. Guimard, M. Nomura, S. Iwamoto, and Y. Arakawa, Nat. Photon. **5**, 91 (2011).
[19] N. I. Zheludev, S. L. Prosvirnin, N. Papasimakis, and V. A. Fedotov, Nat. Photon. **2**, 351 (2008).
[20] P. Berini and I. D. Leon, Nat. Photonics **6**, 16 (2012).
[21] K. Ding and C. Z. Ning, Light: Sci. Appl. **1**, e20 (2012).
[22] O. Hess, J. B. Pendry, S. A. Maier, R. F. Oulton, J. M. Hamm, and K. L. Tsakmakidis, Nat. Mater. **11**, 573 (2012).
[23] O. Hess and K. L. Tsakmakidis, Science **339**, 654 (2013).
[24] M. A. Noginov, G. Zhu, A. M. Belgrave, R. Bakker, V. M. Shalaev, E. E. Narimanov, S. Stout, E. Herz, T. Suteewong, and U. Wiesner, Nature (London) **460**, 1110 (2009).
[25] R. F. Oulton, V. J. Sorger, T. Zentgraf, R. M. Ma, C. Gladden, L. Dai, G. Bartal, and X. Zhang, Nature (London) **461**, 629 (2009).
[26] M. T. Hill, M. Marell, E. S. P. Leong, B. Smalbrugge, Y. C. Zhu, M. H. Sun, P. J. van Veldhoven, E. J. Geluk, F. Karouta, Y. S. Oei, R. Notzel, C. Z. Ning, and M. K. Smit, Opt. Express **17**, 11107 (2009).

[27]M. P. Nezhad, A. Simic, O. Bondarenko, B. Slutsky, A. Mizrahi, L. Feng, V. Lomakin, and Y. Fainman, Nat. Photon. **4**, 395 (2010).
[28]J. H. Lee, M. Khajavikhan, A. Simic, Q. Gu, O. Bondarenko, B. Slutsky, M. P. Nezhad, and Y. Fainman, Opt. Express **19**, 21524 (2009).
[29]K. Yu, A. Lakhani, and M. C. Wu, Opt. Express **18**, 8790 (2010).
[30]R. M. Ma, R. F. Oulton, V. J. Sorger, G. Bartal, and X. Zhang, Nat. Mater. **10**, 110 (2011).
[31]J. B. Khurgin and G. Sun, Opt. Express **20**, 15309 (2012).
[32]A. E. Siegman, *Lasers* (University Science Books, Mill Valley, CA, 1986).
[33]X. Jiang and C. M. Soukoulis, Phys. Rev. Lett. **85**, 70 (2000).
[34]P. Bermel, E. Lidorikis, Y. Fink, and J. D. Joannopoulos, Phys. Rev. B **73**, 165125 (2006).
[35]A. Fang, Th. Koschny, and C. M. Soukoulis, Phys. Rev. B **82**, 121102(R) (2010).
[36]S. Wuestner, A. Pusch, K. L. Tsakmakidis, J. M. Hamm, and O. Hess, Phys. Rev. Lett. **105**, 127401 (2010).
[37]J. M. Hamm, S. Wuestner, K. L. Tsakmakidis, and O. Hess, Phys. Rev. Lett. **107**, 167405 (2011).
[38]Z. Huang, Th. Koschny, and C. M. Soukoulis, Phys. Rev. Lett. **108**, 187402 (2012).
[39]S. Wuestner, A. Pusch, K. L. Tsakmakidis, J. M. Hamm, and O. Hess, Philos. Trans. R. Soc. London, Ser. A **369**, 3525 (2011).
[40]H. E. Türeci, A. D. Stone, and B. Collier, Phys. Rev. A **74**, 043822 (2006).
[41]M. I. Stockman, J. Opt. **12**, 024004 (2010).
[42]A. Cerjan, Y. Chong, L. Ge, and A. D. Stone, Opt. Express **20**, 474 (2011).